On Global Initialization of the Primitive Equations: Part II. The Divergent Component of the Horizontal Wind[1]

DAVID D. HOUGHTON

Dept. of Meteorology, University of Wisconsin, Madison

AND DAVID P. BAUMHEFNER AND WARREN M. WASHINGTON

National Center for Atmospheric Research,[2] Boulder, Colo.

(Manuscript received 16 December 1970)

ABSTRACT

The problem of obtaining initial values for vertical motion and the divergent component of horizontal velocity is examined for a global primitive equation model. Only diagnostic methods are considered, the emphasis being on uniform application over the globe rather than a high degree of accuracy. Results show that a very simple diagnostic equation similar in form to the omega equation provides for realistic values of vertical motion in high and middle latitudes and smooth variations across tropical latitudes. In terms of prediction accuracy, no improvement is noted by using the computed initial vertical motions instead of zero for the initial vertical motions in a six-layer, 5° mesh model. In both cases unrealistic oscillations occur during the first 12 hr.

1. Introduction

This paper presents the second part of a global initialization study made in conjunction with the General Circulation Model at the National Center for Atmospheric Research (Kasahara and Washington, 1967). The first part (Houghton and Washington, 1969) reported on the initialization for the pressure and the nondivergent component of velocity. This second paper discusses the initialization for vertical motion and the divergent component of horizontal wind velocity.

The emphasis here is on establishing a method that can be applied uniformly over the entire globe. Accuracy requirements for the initialization procedures are limited because the present numerical model lacks many refinements and has coarse resolution in the horizontal and vertical. This is especially true for the equatorial region. Accordingly, only simple diagnostic approaches are considered.

A diagnostic equation of long standing for the divergent component of velocity is the so-called omega equation [see, for example, Thompson (1961)]. This, along with some form of the balance equation, is the diagnostic part of the prediction system for a balanced model in pressure coordinates. When pressure-coordinate, primitive equation models for middle and high latitudes were developed, the omega equation became a useful initialization equation for large-scale vertical motions. This diagnostic equation is formed by combining the vorticity equation and the first law of thermodynamics using the geostrophic relation to eliminate time derivatives. Phillips (1960) derived a comparable diagnostic equation for the homogeneous fluid model with a free upper boundary. Charney (1963) obtained a set of equations which led to a comparable relationship for a z-coordinate model. Krishnamurti (1968a) discussed a more accurate form of the omega equation. In his formulation the balance equation—and not the simple geostrophic equation—is used to eliminate time derivatives between the vorticity equation and the first law of thermodynamics; in addition, many terms ordinarily ignored on the basis of quasi-geostrophic scaling are retained. The methods which do not explicitly contain the geostrophic velocity such as Krishnamurti's are solvable across the equator although little is known about the resultant accuracy in such cases.

In an attempt to make the initializing scheme more compatible with the prediction model in terms of truncation errors, time-iterative methods have been proposed by Miyakoda and Moyer (1968) and Nitta and Hovermale (1969) which use some of the prediction equations themselves. Such an approach is referred to by Smagorinsky (1969) when he calls for the use of the information in all four dimensions to most properly assimilate or initialize data into a numerical model. Some tests have been made with these models but none which even indicate that they are mathematically convergent over all parts of the globe or an improvement over much simpler methods. In fact, Økland (1970) has recently shown that time-iterative schemes

[1] Research was partially supported by the Atmospheric Sciences Section, National Science Foundation, under Grant GA-12112.

[2] The National Center for Atmospheric Research is sponsored by the National Science Foundation.

may not handle certain internal gravity wave modes which are common to most multi-layered models.

The present investigation includes testing the computed initial conditions in a prediction experiment, whereas no tests were included in Part I of this study. [Tests for that part are given in a paper by Baumhefner (1970).] The various diagnostic systems possible in z coordinates are presented in Section 2. In Section 3 these are analyzed and the most suitable scheme identified. Section 4 contains actual calculations for vertical motion from real global data. Finally, in Section 5 forecasts are made with the general circulation model and the effects of including vertical motions in the initial conditions are discussed.

2. Formulating the diagnostic equations

In this section we form diagnostic expressions for vertical motion and horizontal divergence. For the purposes of the discussion we assume an adiabatic and inviscid fluid in a Cartesian coordinate system. In pressure coordinates the equations contain only two explicit local time derivatives offering only one way in which to eliminate them. In z coordinates there are four explicit local time derivatives giving a choice in how to eliminate them.

The three basic equations for forming the diagnostic relationships are the quasi-geostrophic vorticity equation,

$$\underset{1a}{\frac{\partial\zeta}{\partial t}}+\underset{1b}{\mathbf{V}\cdot\nabla\zeta}+\underset{1c}{f\nabla\cdot\mathbf{V}}+\underset{1d}{\beta v}=0, \tag{2.1}$$

the continuity equation,

$$\underset{2a}{\frac{\partial\rho}{\partial t}}+\underset{2b}{\mathbf{V}\cdot\nabla\rho}+\underset{2c}{w\frac{\partial\rho}{\partial z}}+\underset{2d}{\rho\nabla\cdot\mathbf{V}}+\underset{2e}{\rho\frac{\partial w}{\partial z}}=0, \tag{2.2}$$

and the first law of thermodynamics,

$$\underset{3a}{\frac{\partial\rho}{\partial t}}+\underset{3b}{\mathbf{V}\cdot\nabla\rho}+\underset{3c}{w\frac{\partial\rho}{\partial z}}-\underset{3d}{\frac{1}{c^2}\frac{\partial p}{\partial t}}-\underset{3e}{\frac{\mathbf{V}\cdot\nabla p}{c^2}}-\underset{3f}{\frac{w}{c^2}\frac{\partial p}{\partial z}}=0. \tag{2.3}$$

Each term is labeled to facilitate the discussion to follow. Variables are defined as follows:

- z vertical coordinate
- t time
- $\mathbf{V}$ horizontal velocity vector
- v north-south component of velocity
- w vertical component of velocity
- ζ vertical component of vorticity
- p pressure
- ρ density
- f Coriolis parameter
- β latitudinal derivative of f
- ∇ horizontal del operator
- c^2 speed of sound squared, equal to $\gamma p/\rho$, where γ is the ratio of specific heats (1.4 for air)

The following equations are used in combining time derivatives: the geostrophic relationship,

$$\zeta=\frac{1}{\rho f}\nabla^2 p, \tag{2.4}$$

where f is assigned constant in (2.4), and the hydrostatic equality,

$$\frac{\partial p}{\partial z}=-\rho g, \tag{2.5}$$

where g is the acceleration of gravity.

Following the scale analysis of Charney (1963), it may be shown that (2.1) is accurate to 10% even in the equatorial region for motions of large vertical scale, i.e., for $\mathrm{Ri}=\mathrm{O}(100)$. In pressure coordinates, the continuity equation contains no explicit time derivatives and the first law of thermodynamics contains only one, i.e., that equivalent to term 3a.

There are three ways in which to combine these equations retaining information from all and ending up with a diagnostic system. These are outlined briefly below.

a. Method A

Ignore terms 2a, 2b, 2c, 3d and 3e; then eliminate $\nabla\cdot\mathbf{V}$ from (2.1) using (2.2); and equate 1a and 3a using (2.4) and (2.5), taking ρ and f to be constant to any additional differentiations. If a stability parameter

$$\sigma=\frac{g}{\rho}\left(\frac{\partial\rho}{\partial z}-\frac{1}{c^2}\frac{\partial p}{\partial z}\right)$$

is defined, the resultant equation is

$$\nabla^2\sigma w-f^2\frac{\partial^2 w}{\partial z^2}=-\frac{g}{\rho}\nabla^2(\mathbf{V}\cdot\nabla\rho)-\frac{\partial}{\partial z}[\mathbf{V}\cdot\nabla(\zeta+f)]. \tag{2.6}$$

The approximations made apply to synoptic-scale motions with the additional assumption that term 2c can be ignored. Scale analysis suggests that terms 3d and 3e which were ignored are the same order of magnitude as any of the other terms in (2.3). Another major approximation was ignoring $\partial\rho/\partial z$ when (2.4) was differentiated with respect to z. Of course (2.4) becomes subject to large error in the equatorial region. We chose this simple derivation to show an equation which is almost equivalent in form to the standard omega equation (Thompson, 1961).

b. Method B

Equate terms 2a, 2b and 2c to 3a, 3b and 3c and thereby combine (2.2) and (2.3); Equate 1a and 3d using (2.4) to combine (2.1) and (2.3), ignoring variations in c^2 and ρ when operated on by ∇^2. The final diagnostic equation is

$$\nabla^2(\nabla\cdot\mathbf{V})-\frac{f^2}{c^2}(\nabla\cdot\mathbf{V})=\frac{g}{c^2}\nabla^2 w-\nabla^2\frac{\partial w}{\partial z}$$
$$-\frac{1}{\rho c^2}\nabla^2(\mathbf{V}\cdot\nabla p)+\frac{f}{c^2}\mathbf{V}\cdot\nabla(\zeta+f). \quad (2.7)$$

This method involves fewer large approximations than Method A.

The diagnostic equation (2.7) contains two unknown quantities, w and $\nabla\cdot\mathbf{V}$. The horizontal divergence is also an unknown because the only horizontal velocity which can be prescribed in (2.7) is either the geostrophic or nondivergent velocity, neither of which give a realistic horizontal divergence. Another independent equation must be found from the original set (2.1)–(2.3). This is the Richardson equation derived from (2.2) and (2.3) using (2.5) which is part of the NCAR model (see Kasahara and Washington, 1967) and is a well-posed second equation for this diagnostic system.

c. Method C

Combine (2.2) and (2.3) by equating terms 2a and 3d using (2.5); combine (2.1) and (2.3) by equating terms 1a and 3a using (2.4) and (2.5). Again we ignore variations in c^2, ρ and f when subject to additional differentiation. The final diagnostic equation is

$$\nabla^2(\nabla\cdot\mathbf{V})-\frac{f^2c^2}{g^2}\frac{\partial^2}{\partial z^2}(\nabla\cdot\mathbf{V})=\frac{fc^2}{g^2}\frac{\partial^2}{\partial z^2}[\mathbf{V}\cdot\nabla(\zeta+f)]$$
$$+\frac{c^2}{\rho g}\nabla^2\frac{\partial}{\partial z}\left(\mathbf{V}\cdot\nabla\rho+w\frac{\partial\rho}{\partial z}\right)-\frac{1}{\rho g}\nabla^2\left(\frac{\partial\mathbf{V}}{\partial z}\cdot\nabla p\right). \quad (2.8)$$

This equation contains the two unknowns, w and $\nabla\cdot\mathbf{V}$, so again the Richardson equation is necessary to make the system solvable.

All of the methods discussed may be applied over the entire globe, except the poles, if the forcing function in each has no terms that are proportional to $1/f$. This means that the horizontal velocity which appears must be a nondivergent velocity instead of the geostrophic velocity. For large-scale motions the error in the nondivergent velocity is inversely proportional to the product of the Richardson and Rossby numbers, whereas the error in the geostrophic velocity is proportional to the Rossby number (Charney, 1963). Even with well-behaved forcing functions, it still must be recognized that the geostrophic relation (2.4) has been used in all the derivations so that none of the methods maintain any accuracy close to the equator. For improvement, it is necessary to use the complete balance relationship in place of the geostrophic conditions (e.g., Krishnamurti, 1968a).

3. Analysis of the diagnostic methods

Method A is an appealing system because it involves only one equation. Several large approximations in its derivation raise questions about the accuracy of the solution. Method B appeals because it is of only first order in vertical differentiation similar to the prediction equations and it uses one of the equations of the prediction model. On the other hand, scale analysis indicates that the first, third and fourth terms in (2.7) are one order of magnitude larger than the other terms so the suitability of this equation, and thus of Method B, is uncertain. Method C was not considered for further study because it contains fourth-order derivatives which make it less compatible in terms of finite differencing with the prediction equations than the other two methods.

A linear beta-plane channel model was used to test and compare Methods A and B. The forcing function was constructed from a zonal geostrophic flow combined with a wave pattern of a single prescribed wavenumber in x, the east-west coordinate. The linearized balance equation was used to give the proper pressure and nondivergent velocity distribution in the wave. Diabatic and frictional effects were ignored.

For a two-layer model with a typical synoptic-scale wave in the middle latitudes when both Methods A and B converged, the phase of the computed vertical motions agreed well but the magnitudes consistently differed. Method A gave magnitudes about 1 cm sec^{-1} while those of Method B were about half as large. Method A gave magnitudes closer to those normally considered typical of large-scale motions. In another comparison using real data in a global two-layer model, similar results were obtained. The computed phase again agreed between the two methods but the magnitudes differed; Method A magnitude extremes were typically 2 cm sec^{-1} and those of Method B were 0.75 cm sec^{-1}, as compared with 3–4 cm sec^{-1} generated by the two-layer general circulation numerical model.

Further experimentation with the linear channel models demonstrated that Method B was only a marginally convergent system. In the two-layer model when smaller scale waves or an equatorial beta plane was simulated, Method B did not converge. With a four-layer model (same total height as the two-layer model) Method B never converged.

A detailed convergence analysis was made for Method B. The error equations for the finite-difference system were formulated and then combined by assuming periodic variations of the errors in both horizontal directions. The resulting error equation is

$$\boldsymbol{\varepsilon}^{\nu+1}=\mathbf{M}\boldsymbol{\varepsilon}^{\nu}, \quad (3.1)$$

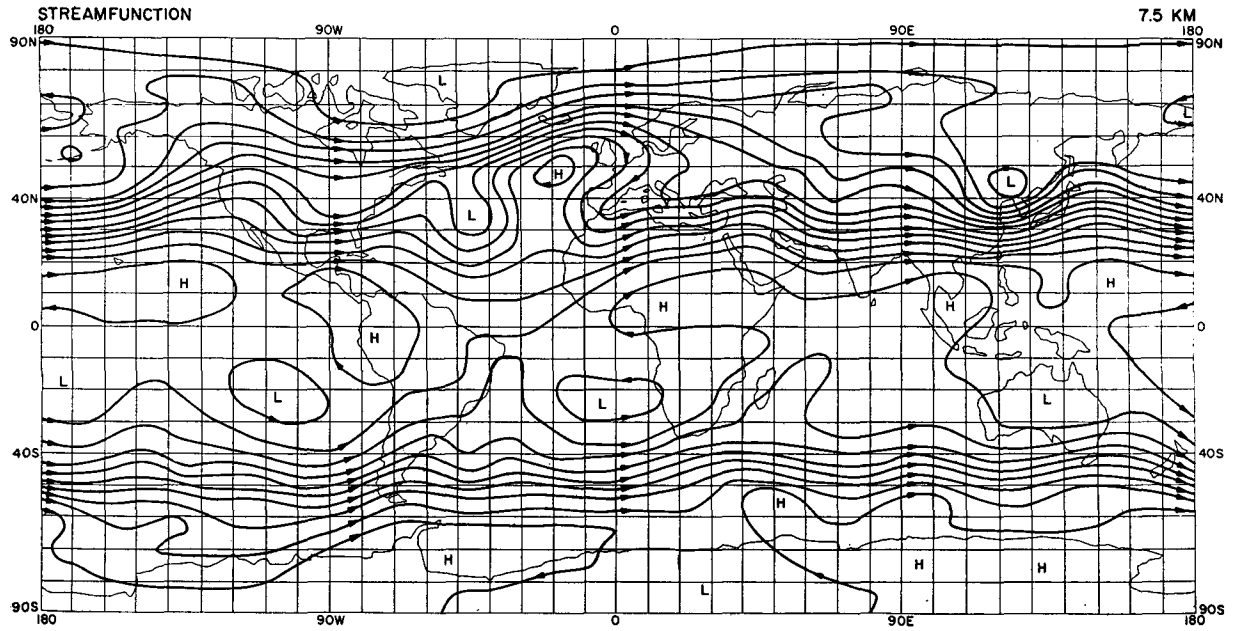

FIG. 1. Streamfunction at 7.5 km for 1200 GMT 15 January 1958.

where $\boldsymbol{\varepsilon}$ is a column matrix of the errors in w at all the grid points in a vertical column, $\mathbf{M}$ is a square and real matrix, and ν refers to the iteration cycle. The norm of $\mathbf{M}$ must be less than unity in order for $\boldsymbol{\varepsilon}$ to become vanishingly small, as $\nu \rightarrow \infty$, i.e., for the system to converge.

A necessary condition for convergence is that the magnitude of all the eigenvalues be less than one. Since the matrix is diagonally dominant, the rate of convergence or the multiplication factor for the errors is given approximately by the magnitude of the largest eigenvalue.

The multiplication factor was computed for an atmosphere 12 km in height for various values of static stability, Coriolis parameter, horizontal scales, and number of layers. The multiplication factor was insensitive to variations in the Coriolis parameter and horizontal scales, being affected in the third significant digit only; nevertheless, it was smaller (implying better convergence) for the larger values of f and horizontal scale. The effect of static stability was large. The more stable the atmosphere the smaller the multiplication factor. For a statically unstable atmosphere, the multiplication factor exceeded unity, implying that the Method B iteration scheme would not converge. As the number of layers was increased, the multiplication factor came closer and closer to unity. For the static stability of the standard atmosphere with representative values of f and the horizontal scales, the multiplication factors were approximately 0.91, 0.96, 0.98, 0.985 and 0.99 for 2, 3, 4, 5 and 6 layers, respectively. These compare to a typical value of 0.60 for Method A. The poor convergence properties of Method B are evident.

In practice, Method B is likely to be less convergent than indicated above. For the four-layer channel model, computation of the multiplication factor at each grid position in the y direction from the values of pressure and density used gave values >1 at some positions, in agreement with the results of attempted solution. However, for the two-layer model, some calculations did diverge when the computed multiplication factor was less than one everywhere. It is likely that truncation errors in the horizontal finite differencing accounts for this discrepancy. Method B may be solvable for a two-layer model but it is definitely unsuitable for models with finer vertical resolution. Furthermore, even when it is solvable, the computed values are not as realistic as those of Method A.

4. Calculation of the initial conditions for a primitive equation model

The analysis in the previous section demonstrated that of the three diagnostic formulations only Method A is feasible for general initialization of vertical motion. In order to test the usefulness of obtaining a complete three-dimensional structure of the velocity field, it was decided to incorporate Method A into a set of diagnostic equations that determine a balanced initial state for prediction.

The initial nondivergent, horizontal velocity field was calculated from the mixed-balance equation method as described by Houghton and Washington (1969) using global data of 1200 GMT 15 January 1958.

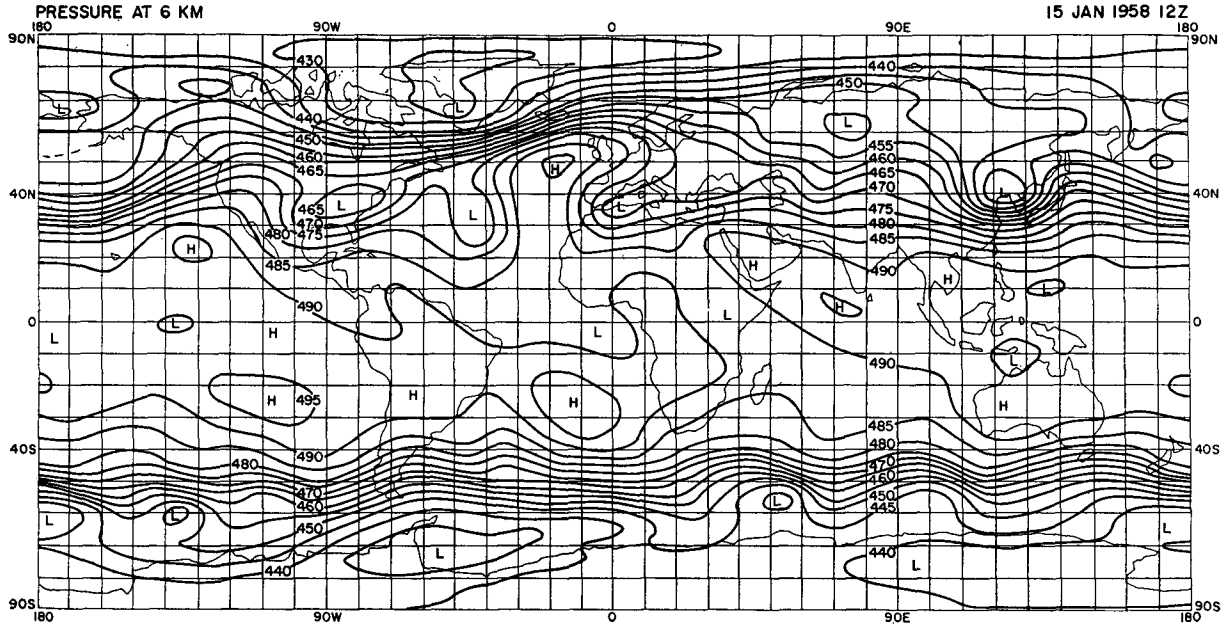

FIG. 2. Modified pressure (mb) at 6 km for 1200 GMT 15 January 1958. Contour interval is 5 mb.

The scheme utilizes the observed pressure in mid-latitudes and the observed velocity in the tropics. The solution by this method is shown in Fig. 1. In this set of diagnostic equations the mass fields in the tropics must be re-calculated by use of an inverted form of the balance equation. A problem arises, due to the vertical staggering of the atmospheric variables in the model, when the balanced pressures are obtained at the velocity levels. Therefore, in order to transform the pressure to the standard levels, a least-squares fit between the observed pressure and the pressure computed by the balance equation is made. The mass field constructed from this procedure is shown in Fig. 2. As can be seen from the illustrations there is a strong correlation between the patterns of ψ and p even in tropical regions.

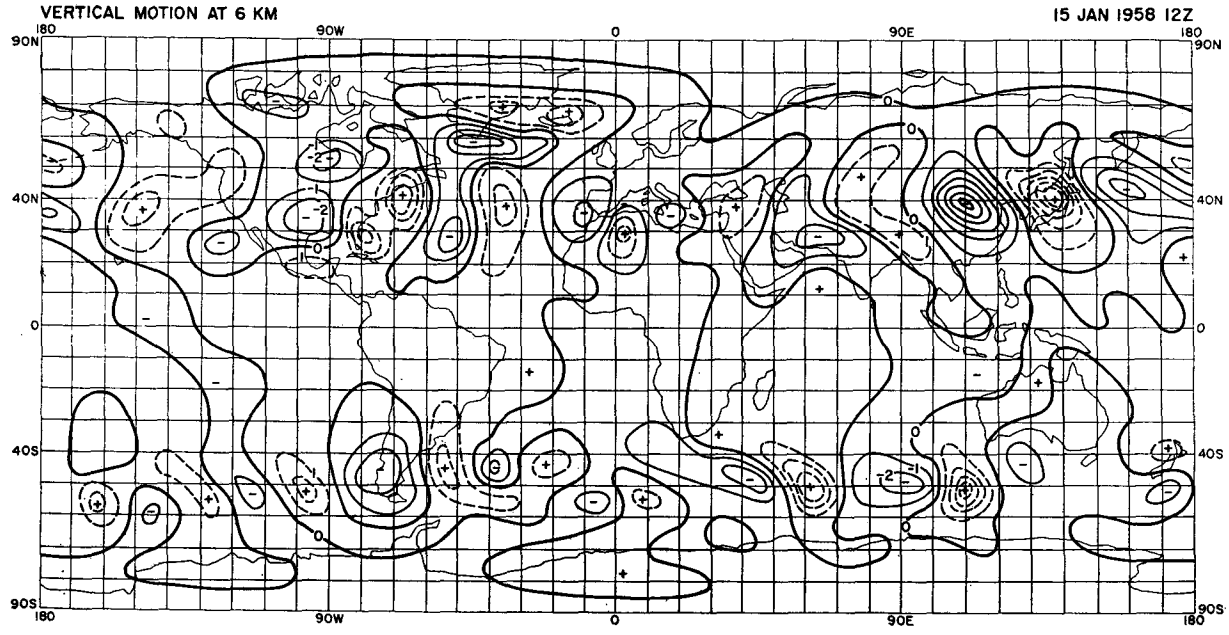

FIG. 3. Calculated vertical motion (cm sec^{-1}) at 6 km for 1200 GMT 15 January 1958. Heavy solid line divides rising and sinking regions. Dashed lines indicate rising air; light solid lines indicate sinking air. Contour interval is 1 cm sec^{-1}.

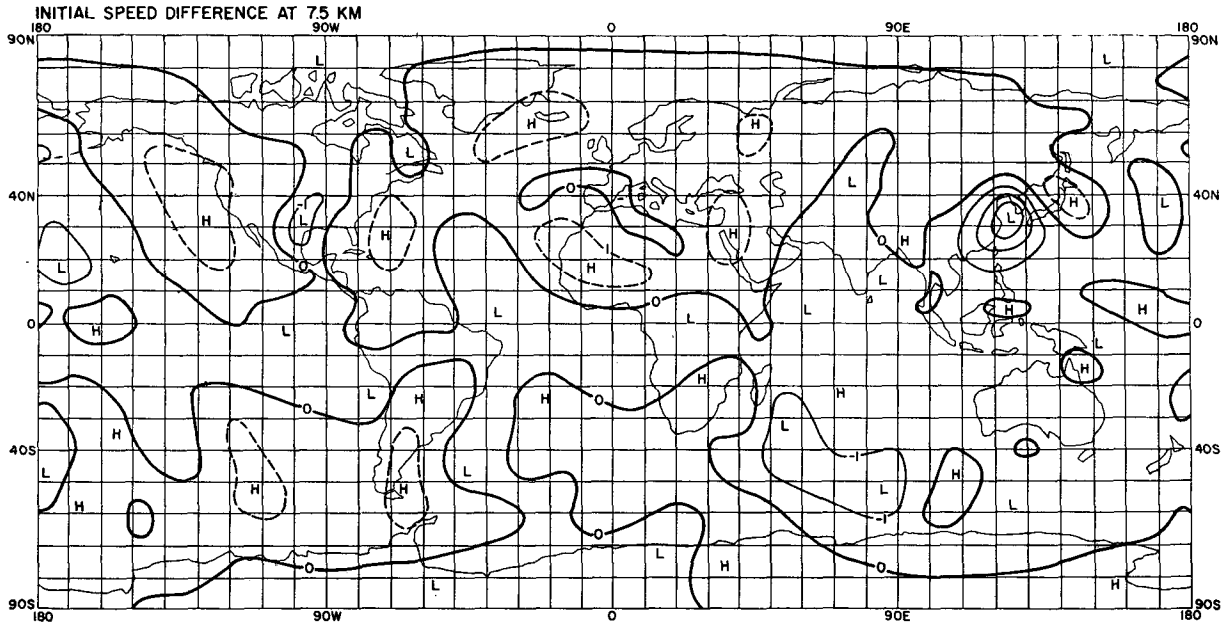

FIG. 4. Initial speed difference (m sec^{-1}) at 7.5 km between divergent and nondivergent initial states. Heavy solid line equals no difference. Dashed lines indicate divergent wind speed less than nondivergent wind; light solid lines indicate divergent wind speed greater than nondivergent wind. Contour interval is 1 m sec^{-1}.

Using these fields as input to Method A, computations of the vertical motion w were made for a six-layer model. Eq. (2.6) was first written in spherical coordinates which for the degree of approximation involved in the method and the domain where it is applied means just replacing Cartesian operators with the corresponding spherical operators. For boundary conditions at the lower and upper boundary, $w=0$. The static stability was set constant at each layer (troposphere: $\sigma=1.4\times10^{-4}$ sec^{-2}; stratosphere: $\sigma=40\times10^{-4}$ sec^{-2}). The result of computing vertical motion from Method A is seen in Fig. 3. The average amplitude of a dipole of vertical velocity in the mid-latitudes of both hemispheres is of the order of ±3 cm sec^{-1}. The maximum amplitude approaches 7 cm sec^{-1} of rising motion for an intense system on the coast of Asia. The tropical region exhibits

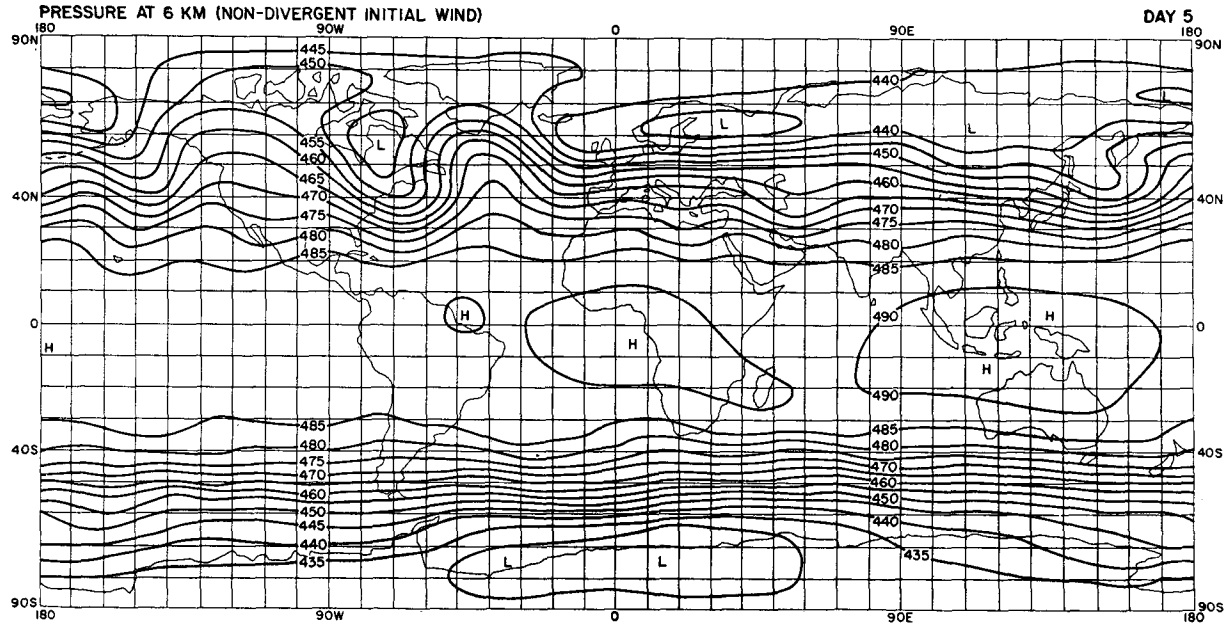

FIG. 5. Pressure forecast (mb) at 5 days at 6 km starting from a nondivergent initial state. Contour interval is 5 mb.

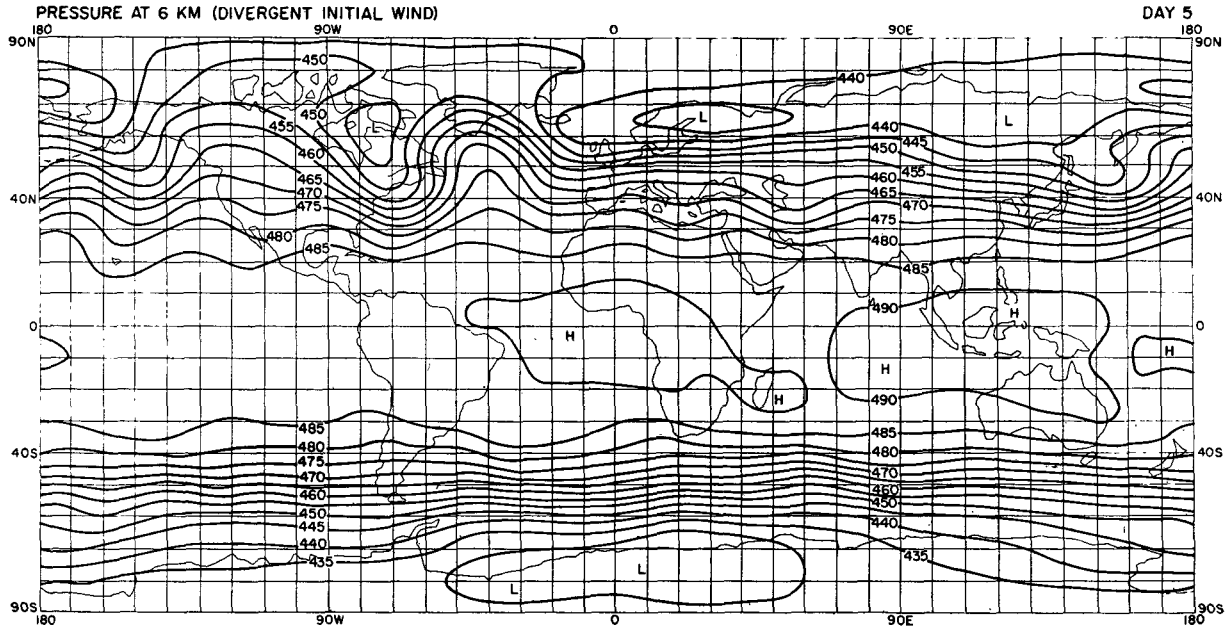

FIG. 6. Pressure forecast (mb) at 5 days at 6 km starting from a divergent initial state. Contour interval is 5 mb.

no organized area of vertical velocity with the magnitudes being much less than 1 cm sec^{-1} throughout. These values appear to be the same order of magnitude as those of Krishnamurti (1968b) and Baumhefner (1968).

5. Forecast experiment

The initial conditions described in Section 4 were used to start two prediction experiments: 1) a control case in which just the nondivergent wind of the initialization technique was used as the initial velocity,

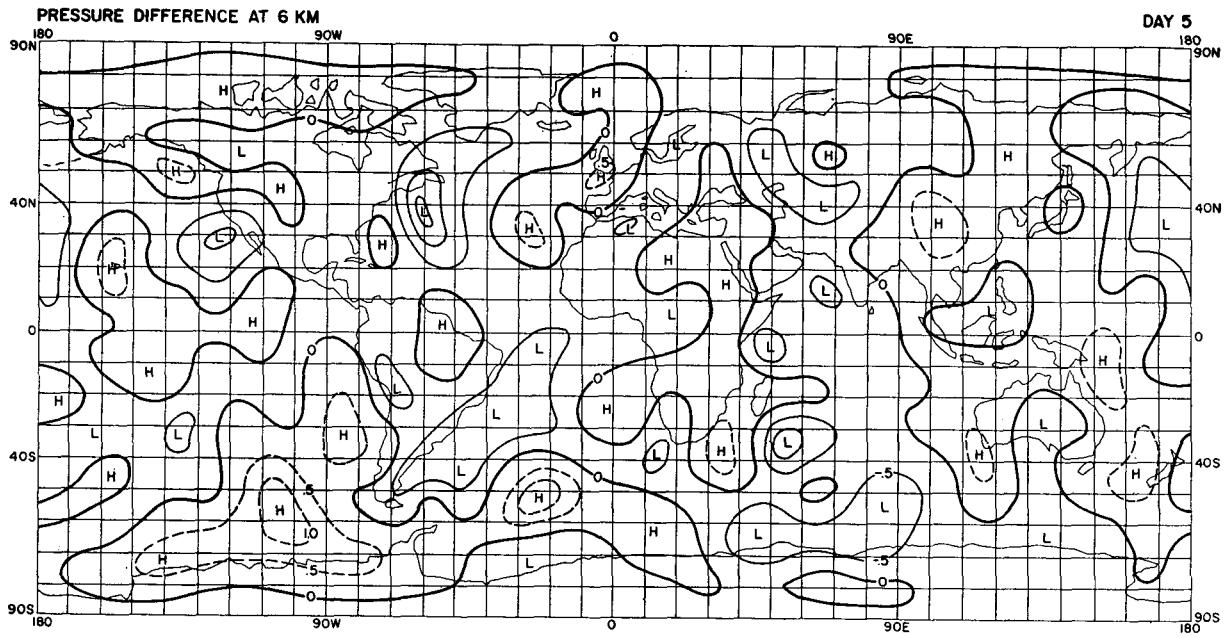

FIG. 7. Difference in pressure forecasts shown in Figs. 5 and 6. Heavy solid line equals no difference. Dashed lines indicate divergent wind pressure less than nondivergent wind pressure; light solid lines indicate divergent wind pressure greater than nondivergent wind pressure. Contour interval is 0.5 mb.

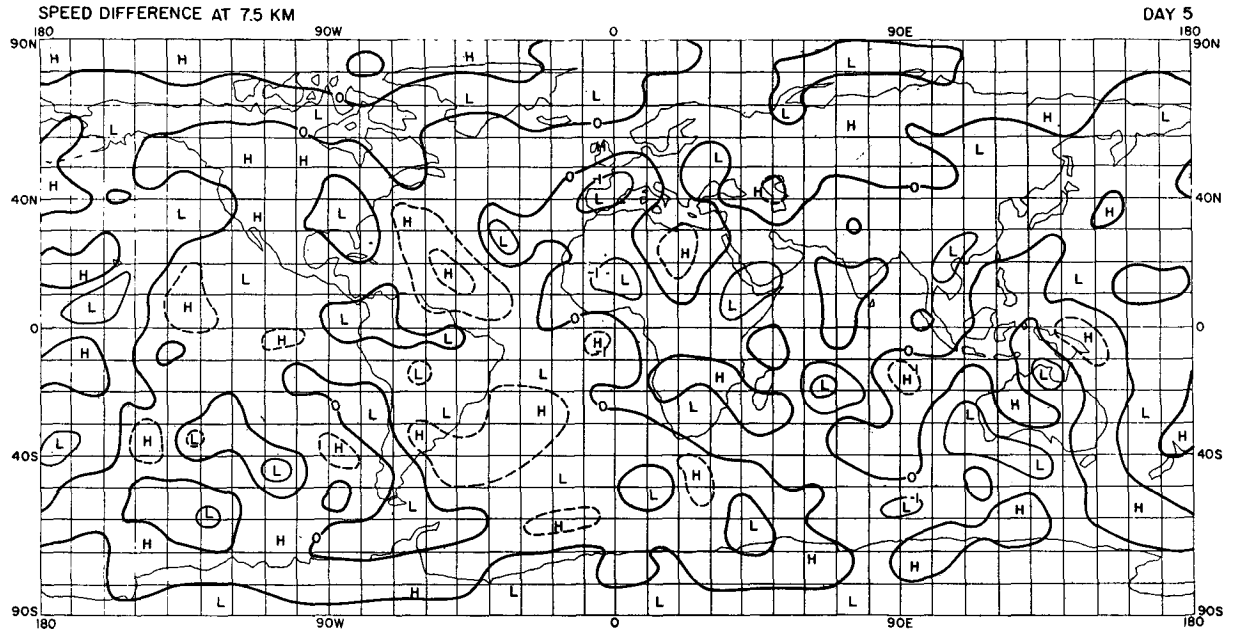

FIG. 8. Difference in speed forecast at 7.5 km at 5 days. Otherwise, same as Fig. 4.

and 2) a test case run with the divergent part of the wind field calculated from the vertical motion of Method A and added to the initial nondivergent wind. The pressure fields are exactly the same for both cases. Only small changes in the wind fields were noted when the initial states of both experiments are compared. The magnitude of these differences in the speed field at 7.5 km (Fig. 4) are the order of ± 1 m sec^{-1}, with the largest being 4 m sec^{-1} on the coast of Asia.

Both forecasts were carried out to 5 days with a six-layer, 5° mesh primitive equation model. The results for the pressure at 6 km can be seen in Figs. 5 and 6. The effect of adding a divergent component to the initial wind field is not significant in the forecast, with only small differences (Fig. 7) between the two experiments at the end of 5 days. The same can be said for the other levels in the model; the largest difference between the two surface pressure forecasts (not shown) was just over 2 mb. It appears, from examining the difference maps (Figs. 7 and 8) of the pressure and wind speed, that the spatial distribution of change is not organized in any particular way after 5 days. Of course, initially, the most pronounced regions of change were in the vicinity of large vertical motion shown in Fig. 3. The initial difference in the wind field (Fig. 4) has not grown appreciably in the course of the forecast, and at 5 days (Fig. 8) the differences do not exceed ± 3 m sec^{-1}.

In order to examine more closely the behavior of the model when the initial divergent wind is calculated from Method A, a plot of the vertical motion and surface pressure at a particular point was constructed from information at each iteration in the forecast. The location of this point comparison is at 40N, 140E in an area of strong rising motion on the coast of Asia. These plots are illustrated in Figs. 9 and 10.

The case in which the initial vertical motion was absent recovers in 4–5 hr to approximately the value calculated by Method A as part of a large oscillation. After the low pressure center passes the grid point (refer to Fig. 10) at 8 hr, the vertical motion drops off with only a small oscillation. When initial divergence is included, a large oscillation occurs in the first 8 hr of the forecast opposite in phase to that occurring in the case without initial vertical motion. After 12 hr the two cases are nearly the same, with deviations

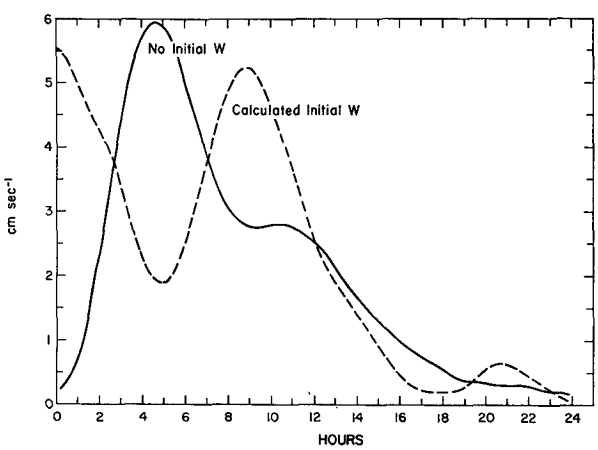

FIG. 9. Comparison of the vertical velocity (cm sec^{-1}) at 40N, 140E for the first 24-hr period. Solid line shows the vertical velocity with no initial divergence; dashed line with initial divergence.

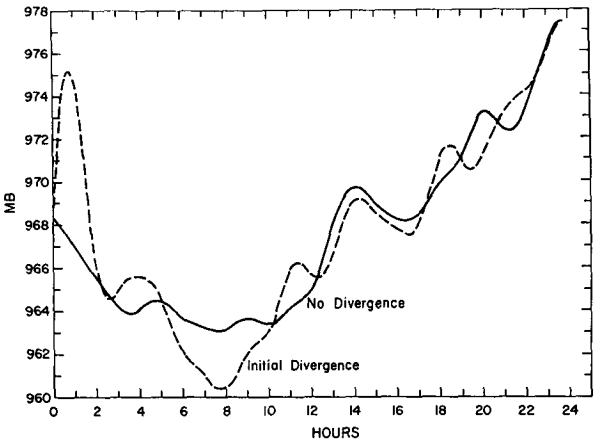

FIG. 10. Comparison of the surface pressure (mb) at 40N, 140E for the first 24-hr period. Solid line illustrates behavior of pressure with no initial divergence; dashed line with initial divergence.

of less than 1 cm sec^{-1}. The surface pressure plot (Fig. 10) exhibits somewhat different characteristics than the vertical motion. The "no-divergence" case reacts in a relatively smooth manner with a small gravity-acoustic wave mode superimposed on the synoptic mode, whereas the "initial divergence" case shows several significant oscillations of the order of 5 mb in the first 12 hr. During the latter part of the first day the two curves begin to approach a common value as in the case of the vertical motion. It appears that both methods give significant deviations from realistic atmospheric conditions for the first 12 hr.

6. Conclusions

This paper has attempted to examine the feasibility of calculating the initial divergent component of the velocity over the entire globe from a diagnostic relationship and to assess its usefulness in short-range weather prediction. The following conclusions may be stated:

1) Method A, a simple omega-equation-type relationship, gives reasonable patterns and magnitudes of vertical motion in the middle latitudes.

2) The addition of an initial divergent wind had a small effect initially on the numerical prediction but after 12 hr no appreciable or systematic differences were observed.

3) The gravity-acoustic wave mode did not appear to be reduced during the first 12 hr by including the initial vertical motion calculated from Method A.

It may be that the poor model resolution for the small scale inherent in the vertical motion field contributed significantly to the apparent lack of any improvement in the forecast patterns by trying to initialize for vertical motion. It is well known that large errors in phase speed can occur under such conditions. We plan to carry out further experiments with a higher resolution model (2.5° mesh) to see what role resolution has in this problem.

Acknowledgments. The authors wish to thank Gerry Browning for the excellent job in programming Method A and an improved version of the nondivergent wind calculation, and Linda Thiel for running the experiments on the NCAR Control Data Corporation 6600 Computer. Richard Wobus assisted with the linear analysis for convergence.

REFERENCES

Baumhefner, D. P., 1968: Application of a diagnostic numerical model to the tropical atmosphere. *Mon. Wea. Rev.*, **96**, 218–228.

——, 1970: Global real-data forecasts with the NCAR two-layer general circulation model. *Mon. Wea. Rev.*, **98**, 92–99.

Charney, J. G., 1963: A note on large-scale motions in the tropics. *J. Atmos. Sci.*, **20**, 607–609.

Houghton, D., and W. Washington, 1969: On global initialization of the primitive equations: Part I. *J. Appl. Meteor.*, **8**, 726–737.

Kasahara, A., and W. M. Washington, 1967: NCAR global general circulation model of the atmosphere. *Mon. Wea. Rev.*, **95**, 389–402.

Krishnamurti, T. N., 1968a: A diagnostic balance model for studies of weather systems of low and high latitudes, Rossby number less than 1. *Mon. Wea. Rev.*, **96**, 197–207.

——, 1968b: A study of a developing wave cyclone. *Mon. Wea. Rev.*, **96**, 208–217.

Miyakoda, K., and R. W. Moyer, 1968: A method of initialization for dynamical weather forecasting *Tellus*, **20**, 113–128.

Nitta, T., and J. B. Hovermale, 1969: A technique for objective analysis and initialization for the primitive forecast equations. *Mon. Wea. Rev.*, **97**, 652–658.

Økland, H., 1970: On the adjustment toward balance in primitive equation weather prediction models. *Mon. Wea. Rev.*, **98**, 271–279.

Phillips, N. A., 1960: On the problem of initial data for the primitive equations. *Tellus*, **12**, 121–126.

Smagorinsky, J., 1969: Problems and promises of deterministic extended range forecasting. *Bull. Amer. Meteor. Soc.*, **50**, 286–311.

Thompson, P. D., 1961: *Numerical Weather Analysis and Prediction.* New York, The Macmillan Company, 170 pp.